Experimental

General Procedure for Competitive Reduction. Competitive reduction of hexanal and 2-heptanone is described as a representative: one mmol each of hexanal, 2-heptanone, and mesitylene (internal standard) was dissolved in 20 mL of methanol and ethanol (6 : 1 in volume) followed by the addition of 1 drop (*ca.* 0.15 mmol) of *conc* HCl. The mixture was stirred for 30 min at room temperature, and BER (0.94 g, 3 mmol) was added. After 3 h, the GLPC analysis of the mixture on column FFAP showed 96% of 2-heptanol, 2% of 2-heptanone ketal, and 100% of hexanal acetal.

Selective Reduction of Ketoaldehyde 1 to Hydroxyaldehyde 2. Ketoaldehyde[7] **1** (0.50 g, 3 mmol), prepared by ozonolysis of α-pinene in 72% yield[8], was dissolved in 30 mL of methanol and ethanol (6: 1 in volume) followed by the addition of 3 drops of *conc* HCl. The mixture was stirred for 10 min at room temperature, and BER (4.69 g, 15 mmol) was added. After 1 h, BER was removed by filtration. The filtrate was concentrated, and the crude oil (acetal) was dissolved in 20 mL of methylene chloride and hydrolyzed with 2 N HCl. The methylene chloride solution was dried over anhydrous $MgSO_4$, filtered, concentrated, and purified by column chromatography on silica gel (eluted with hexane-EtOAc, 6 : 4) to afford 0.43 g (84%) of hydroxyaldehyde **2** as a yellowish oil: ^{1}H NMR ($CDCl_3$): δ 1.01-1.26 (m, 1H), 1.01 (s, 3H), 1.05 (d, 3H, *J*=6.4 Hz), 1.15 (s, 3H), 1.73-1.87 (m, 1H), 1.94-2.07 (m, 1H), 2.20-2.46 (m, 3H), 3.67-3.75 (m, 1 H), 9.72 (t, 1H, *J*=1.7 Hz); IR (NaCl, neat) 3407, 2871, 2721, 1721, 1462 cm^{-1}; MS m/z (relative intensity) (EI, 70 eV) 155 (1), 137 (1), 100 (38), 98 (14), 85 (100), 69 (55), 43 (16); Anal. Calcd for $C_{10}H_{18}O_2$: C, 70.55; H, 10.66. Found: C, 70.28; H, 10.57.

Aknowledgment. This work was supported by Organic Chemistry Research Center (OCRC) / KOSEF.

References

1. Gemal, A. L.; Luche, J. L. *J. Org. Chem.* **1979**, *44*, 4187.
2. Luche, J. L.; Gemal, A. L. *J. Am. Chem. Soc.* **1979**, *101*, 5848.
3. Gemal, A. L.; Luche, J. L. *Tetrahedron Lett.* **1981**, *22*, 4077.
4. Paradisi, M. P.; Zecchini, G. P.; Ortar, G. *Tetrahedron Lett.* **1980**, *21*, 5085.
5. Yoon, N. M.; Kim, E. G.; Son, H. S.; Choi, J. *Synth. Commun.* **1993**, *23*, 1595.
6. Yoon, N. M.; Park, K. B.; Gyoung, Y. S. *Tetrahedron Lett.* **1983**, *24*, 5367.
7. Spectral data of ketoaldehyde: ^{1}H NMR ($CDCl_3$): δ 0.84 (s, 3H), 1.33 (s, 3H), 1.89-2.05 (m, 2H), 2.03 (s, 3H), 2.35-2.49 (m, 3H), 2.91 (dd, 1H, *J*=9.4, 8.2 Hz), 9.73 (t, 1H, *J*=1.5 Hz); MS m/z (relative intensity) (EI, 70 eV) 168 (M^+, 1), 153 (2), 140 (2), 98 (58), 97 (41), 83 (100), 69 (57), 43 (19).
8. McMurry, J. E.; Bosch, G. K. *J. Org. Chem.* **1987**, *52*, 4885.

Electrochemical Behavior of Iron(II) Chelates-Sodium Dodecyl Sulfate in H_2SO_4 Aqueous Solution

Young Chun Ko, Jongbaik Ree†, and Keun Ho Chung†

Department of Chemistry, Chonnam National University, Kwangju 500-757, Korea
†Department of Chemistry Education, Chonnam National University, Kwangju 500-757, Korea
Received September 5, 1996

Surfactants which possess both a polar or ionic head group and a hydrocarbon chain have been used in a variety of biochemical applications.[1-3] The hydrocarbon chain (hydrophobic part) of surfactants in aqueous solution is directed inward, and the polar head group (hydrophilic part) is directed outward into the bulk polar solvent.[4-6] Thus, micellar assemblies have been extensively utilized in order to apply models for biological membranes[7] and redox processes in biological systems.[8] In the vicinity of a critical micelle concentration (CMC), however the study of ions and organic molecules has received little attention.[9,10]

In this note, the investigation of electrochemical behaviors of two iron(II)chelates, tris(2,2'-bipyridine)iron(II)- and tris(1,10-phenanthroline)iron(II)-sodium dodecyl sulfate (SDS) in H_2SO_4 aqueous solution using cyclic voltammetry (CV) is reported. The behaviors in the vicinity of a CMC is especially addressed. The structure of the double layer around a glassy carbon electrode (GC) resulting from iron chelate-SDS interactions is rationalized using the model proposed by Jaramillo *et al.*[11] Information on iron(II) chelates-SDS interactions comes from considering changes in peak currents and potentials determined by CV. The hydrophobic and electrostatic contribution to micelle association is estimated semi-quantitatively, and the effect of added SDS on iron(II) chelates with varying ligand is compared.

Experiments

Tris(2,2'-bipyridine)iron(II), $Fe(bpy)_3^{2+}$, and tris(1,10-phenanthroline)iron(II), $Fe(ph)_3^{2+}$, were prepared according

to previously reported procedures.[12,13] SDS and H_2SO_4 were obtained from Aldrich and Wako, respectively, and used without further purification. Doubly distilled water was used to prepare all solutions. Glassy carbon disk (Bioanalytical Systems, West Lafayette, in USA) with a geometric area of 0.0788 cm^2 was used as a working electrode. It was polished with 0.05 μm γ alumina/water slurry on a felt surface and then subjected to ultrasonic cleaning for about 2 min. A saturated calomel electrode (SCE) and a platinum mesh were used as a reference electrode and as an auxiliary electrode, respectively. All experiments were performed under a purified nitrogen atmosphere at 25±0.2 °C.

Results and Discussion

Cyclic voltammograms of 1.0 mM $Fe(bpy)_3^{2+}$ in 50 mM H_2SO_4 solution, without and with SDS, are shown in Figure 1. First waves are not shown in the absence of SDS (see Figure 1(a)). Those, however, appeared in the range of 200 to 640 mV when SDS was added (see Figure 1(b-c)), which is considered to be peak formed owing to the electrode response (*via* Eq. (2)) of SDS with Fe^{2+} derived by the decomposition (by means of Eq. (1))[12] of $Fe(bpy)_3^{2+}$.

$$Fe(bpy)_3^{2+} \xrightarrow{\text{in } H_2SO_4} Fe^{2+} + 3bpy \quad (1)$$

$$Fe^{2+}\text{-}(DS^-)_n \rightleftarrows Fe^{3+}\text{-}(DS^-)_n + e^- \quad (2)$$

A blank test, the electrode response (*via* Eq. (2)) of SDS with $FeSO_4$, shows the same peaks. Second waves are redox waves of $Fe(bpy)_3^{3+/2+}$ and voltammetric results are shown with increasing [SDS] in Table 1. In Figure 1 (b-c), sharp spikes in the region A are due to Eq. (3):

$$Fe(bpy)_3^{2+} + 2\ SD^- \text{ (dodecyl sulfate anion)} \rightarrow Fe(bpy)_3(SD)_2 \quad (3)$$

These spikes begin to appear approximately in 1.0 mM SDS and disappear above 4.5 mM.

In the absence of SDS, the oxidation of $Fe(bpy)_3^{2+}$ to $Fe(bpy)_3^{3+}$ takes place at a anodic peak potential (E_{pa}) of 823 mV *vs.* SCE and rereduction of $Fe(bpy)_3^{3+}$ occurs at 775 mV upon scan reversal. The formal potential $E_{1/2}$ taken as the average of Epa and E_{pc} is 799 mV. From values of ΔE_p and i_{pa}/i_{pc} in the absence of SDS, it can be considered that the redox couple is electrochemically quasi-reversible. Here, ΔE_p means E_{pa}-E_{pc} and it shouldn't be confused with the variation of potential on the addition of SDS.

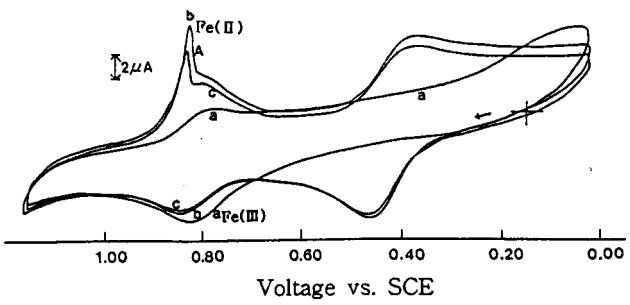

Figure 1. Cyclic voltammograms of 1.0 mM $Fe(bpy)_3^{2+}$ in 50 mM H_2SO_4 with and without SDS at 25.0±0.2 °C. Scan rate=100 mV/s. (a) [SDS]=0.0 mM; (b) [SDS]=3.0 mM; (c) [SDS]=4.0 mM.

In the presence of SDS, E_{pa} of $Fe(bpy)_3^{3+/2+}$ shifts in positive direction compared to the SDS free case. Also, ΔE_p shows a special phenomenon as [SDS] increases. It decreases up to 3.0 mM SDS and increases rapidly above that. On the other hand, Kaifer and Bard[9] proposed that the CMC can be estimated by the shape of the cyclic voltammogram. Thus, in order to see the relation between ΔE_p and CMC, ΔE_p *vs.* -log[SDS] (the solid lines) for the redox couples in Figure 2 were plotted. The intersection of two lines (the solid lines) in Figure 2 is 3.38 mM SDS, which is very near CMC measured by tensiometry (3.24 mM SDS)[14] in Figure 3 (relative error: below 5%). In a similar way, the intersection of two lines on the ΔE_p *vs.* -log[SDS] plot for 1.0 mM $Fe(ph)_3^{3+/2+}$ with SDS in 100 mM H_2SO_4 is 2.47 mM SDS (CMC by tensiometry is 2.56 mM SDS). To confirm this intersection to be CMC, i_{pa}/i_{pc} *vs.* -log[SDS] (the dotted lines) were plotted in Figure 2. This plot also shows the particular picture in the vicinity of 3.5 mM SDS. The i_{pa}/i_{pc} decreases up to this and increases rapidly above this, which implies a specific change has appeared in this region. This indicates that this region shows the biggest change in the CV and is the CMC. Thus, it can be suggested that, for each $Fe(bpy)_3^{3+/2+}$ and $Fe(ph)_3^{3+/2+}$ with SDS in H_2SO_4 aqueous solution, the intersection of two lines of ΔE_p *vs.* log [SDS] plot is the CMC. Oshawa *et al.* reported that the sudden decrease of ΔE_p for osmium(II) chelate with sodium dodecyl sulfate (SDS) in H_2SO_4 aqueous solution poses a puzzling feature.[15]

As mentioned above, CMC exists in the vicinity of a minimal value of ΔE_p. The puzzling feature proposed by them can also therefore be explained by CMC. As shown in Figure 2, the value of ΔE_p decreases linearly with increasing log[SDS] up to CMC, but increases rapidly above that. It is

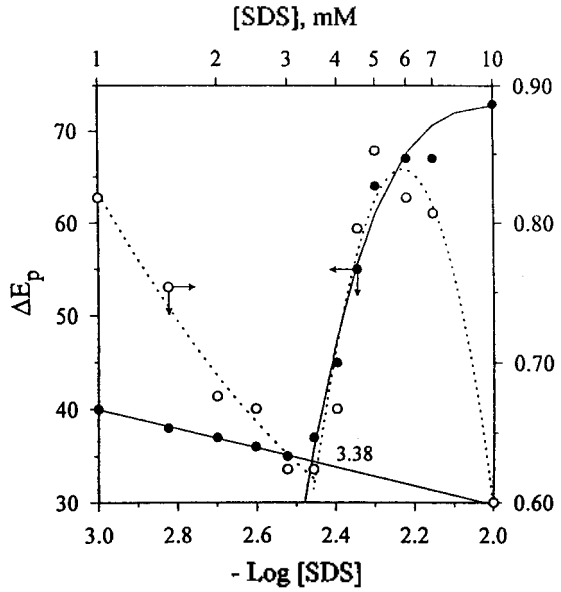

Figure 2. ΔE_p (solid lines) and i_{pa}/i_{pc} (dotted lines) *vs.* -log[SDS] plot for 1.0 mM $Fe(bpy)_3^{2+}$ in 50 mM H_2SO_4. Here, solid lines should be read by left abscissa, and dotted lines by right abscissa.

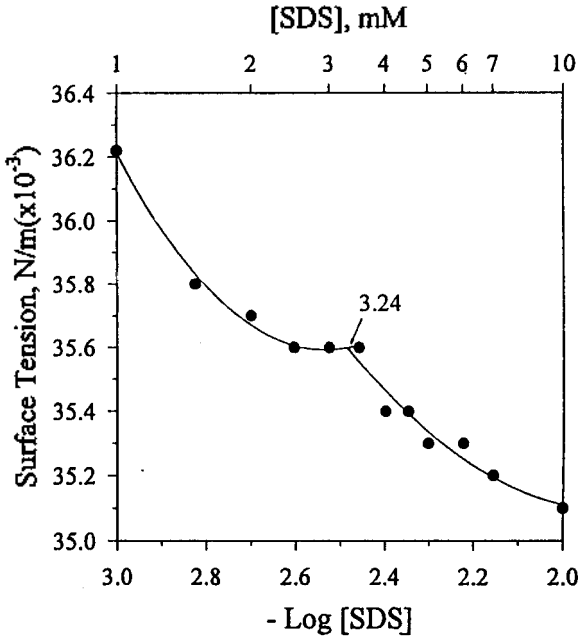

Figure 3. Surface tension *vs.* -log[SDS] plot for 1.0 mM Fe $(bpy)_3^{2+}$ in 50 mM H_2SO_4.

assumed that the added surfactant changes the microscopic environments of the double layer around the electrode by forming monomers up to CMC and micelles above CMC, respectively. SDS provides hydrophobic and hydrophilic environments for the response of $Fe(bpy)_3^{3+/2+}$ to the electrode. $Fe(bpy)_3^{3+/2+}$ interacts not only with ionic head groups of SDS owing to electrostatic coulombic force, but also with the hydrocarbon chain of SDS due to hydrophobic properties. On the other hand, it can be explained that i_{pa}/i_{pc} decreases up to 3.5 mM SDS due to the decrease in the number of $Fe(bpy)_3^{2+}$ species per dodecyl sulfate anion (DS^-) monomer as [SDS] increases to CMC, but increases rapidly to form micelles above CMC (see dotted lines in Figure 2). Continuously after 5.0 mM SDS, i_{pa}/i_{pc} decreases again due to the decrease of the number of $Fe(bpy)_3^{2+}$ species per micelles. According to the model proposed by Jaramillo *et al.*,[11] as [SDS] increases up to CMC, the width of the double layer (*i.e.*, distance to the surface) is narrowed by arranging monomers ($(DS^-)_n$) around the electrode, which speeds up the electron transfer.[11] However, because the screening of the electrode surface by arranging monomers can reduce a response of $Fe(bpy)_3^{2+}$ species, it can also reduce ipa (see Table 1). As [SDS] increases above CMC, micelles are formed gradually. The increase in the number of micelles causes the width of the double layer to increase, which makes the electron transfer slower (*i.e.*, a increase on ΔE_p). Near CMC, monomers around the electrode become dynamic to form micelles. Thus, because the screening of the electrode surface decreases, i_{pa} of $Fe(bpy)_3^{2+}$ species is expected to increase between 3.5 and 4.0 mM SDS rather than 3.0 mM SDS. (As shown in Table 3, i_{pa} of $Fe(ph)_3^{2+}$ species shows an increase in 2.5-3.5 mM SDS rather than 2.0 mM SDS). However, i_{pa} of the former is decreased (see Table 1). This is considered to be because $Fe(bpy)_3^{2+}$ species in H_2SO_4 can be more easily decomposed[12] due to frequent contact between $Fe(bpy)_3^{+2}$ and H_2SO_4 to form micelles. Above that concentration, i_{pa} is decreased continuously but ΔE_p is increased gradually (as also shown in Table 3, for $Fe(ph)_3^{2+}$, i_{pa} is decreased continuously but ΔE_p is increased gradually above 4.0 mM).

Table 1. Electrochemical Data for 1.0 mM $Fe(phy)_3^{2+}$ in 50 mM H_2SO_4 with and without SDS at 25.0±0.2 °C (Voltammogram of the second waves). Scan rate=100 mV/s

[SDS] (mM)	E_{pa} (mV)	ΔE_p (mV)	$E_{1/2}$ (mV)	i_{pa} (μA)	i_{pa}/i_{pc}
0.0	823	48	799	3.42	1.97
1.0	834	40	814	2.60	0.83
1.5	838	38	819	2.72	0.77
2.0	840	37	822	2.54	0.69
2.5	841	36	823	2.62	0.68
3.0	841	35	824	2.50	0.63
3.5	843	37	824	2.32	0.63
4.0	844	45	822	2.26	0.68
4.5	844	55	817	2.02	0.81
5.0	849	64	817	1.92	0.86
6.0	850	67	817	1.66	0.83
7.0	851	67	817	1.84	0.82
10.0	850	73	814	0.72	0.60

$$\begin{array}{ccccc} Fe(bpy)_3^{3+} & + & e^- & \rightleftharpoons & Fe(bpy)_3^{2+} \quad E_f^{0\prime} \\ \uparrow\downarrow K_{+3} & & & & \uparrow\downarrow K_{+2} \\ Fe(bpy)_3^{3+}\text{-}(DS^-)_n & + & e^- & \rightleftharpoons & Fe(bpy)_3^{2+}\text{-}(DS^-)_n \quad E_a^{0\prime} \end{array}$$

Scheme 1.

On the other hand, we can calculate the ratios of the association constant from $E_{1/2}$ by applying Scheme 1.[16] Here, $Fe(bpy)_3^{3+}$ and $Fe(bpy)_3^{2+}$ represent the oxidized and reduced form of the iron complex, and $Fe(bpy)_3^{3+/2+}\text{-}(DS^-)_n$ denotes $Fe(bpy)_3^{3+/2+}$ species associated to DS^-. $E_f^{0\prime}$ and $E_a^{0\prime}$ are the formal potentials of the +3/+2 couple of the iron complex in the free and associated forms, respectively. K_{+3} and K_{+2} are the corresponding association constants for the +3 and +2 ions of iron complex to DS^-. The Nernst equation for the reversible $1e^-$ redox reaction of free and associated species can be written as

$$E_a^{0\prime} - E_f^{0\prime} = 0.059 \log(K_{+2}/K_{+3}) \quad (4)$$

By substituting $E_{1/2}$ in Table 1 to Eq (4), the ratios of equilibrium constants for the association of the +2 and +3 ions of iron complex to DS- can be obtained and are listed in Table 2. Since K_{+2}/K_{+3} is larger than 1, it can be concluded that a reduced form $Fe(bpy)_3^{2+}$ is more easily associated to DS- than an oxidized form $Fe(bpy)_3^{3+}$. Thus, $Fe(bpy)_3^{3+/2+}$ in the presence of SDS is more affected by hydrophobic interactions than by electrostatic interactions.[1,17] However, even though K_{+2}/K_{+3} is larger than 1, i_{pa}/i_{pc} is smaller than 1. This can be explained as $Fe(bpy)_3^{2+}$ species in H_2SO_4 are due either to the decomposition as in Eq. (1) or to micelles formation.

Influence of ligands. Data for the redox reaction of 1.0 mM $Fe(ph)_3^{2+}$ in 100 mM H_2SO_4 solution is shown in Table 3 with increasing [SDS]. In the absence of SDS, the formal potential of $Fe(ph)_3^{2+}$ in 100 mM H_2SO_4 is 824 mV, whilst

Table 2. Ratios of the Association Constants for the $Fe(bpy)_3^{2+}$ and $Fe(bpy)_3^{3+}$ Species to DS⁻ in 50 mM H_2SO_4

[SDS] (mM)	K_{+2}/K_{+3}
1.0	1.80
1.5	2.18
2.0	2.45
2.5	2.55
3.0	2.65
3.5	2.65
4.0	2.45
4.5	2.02
5.0	2.02
6.0	2.02
7.0	2.02
10.0	1.80

Table 3. Electrochemical Data for 1.0 mM $Fe(ph)_3^{2+}$ in 100 mM H_2SO_4 with and without SDS at 25.0±0.2 °C. Scan rate=100 mV/s

[SDS] (mM)	E_{pa} (mV)	ΔE_p (mV)	$E_{1/2}$ (mV)	i_{pa} (μA)	i_{pa}/i_{pc}
0.0	854	60	824	4.78	1.12
1.0	874	60	844	3.90	1.88
1.5	874	36	856	3.62	2.01
2.0	869	20	859	3.20	2.19
2.5	884	9	879	5.00	1.30
3.0	899	21	889	5.14	0.91
3.5	894	34	877	5.74	0.93
4.0	897	41	877	4.61	1.08
4.5	897	46	874	4.52	1.15
5.0	898	50	873	4.18	1.22
6.0	902	54	875	3.96	1.20
7.0	907	58	878	3.70	1.18
10.0	909	63	878	3.18	1.01

that of $Fe(bpy)_3^{2+}$ in 50 mM H_2SO^4 is 799 mV (see Table 1 and 3). This indicates that, even though the concentration of H_2SO_4 in the experiment for $Fe(bpy)_3^{2+}$ is lower than that for $Fe(ph)^{32+}$, $Fe(bpy)_2^{2+*}$ is more unstable than $Fe(ph)^{32+}$ in the experiment.

In the presence of SDS, the formal potential of iron complexes with 2,2'-bipyridine and 1,10-phenanthroline shifts in the positive direction compared to the SDS free case. This indicates that a reduced form of the iron complex is more easily associated to DS- than an oxidized form, because K_{+2}/K_{+3} is larger than 1 (see Table 2). Thus, it can be concluded that both $Fe(bpy)_3^{3+/2+}$ and $Fe(ph)_3^{3+/2+}$ are more affected by hydrophobic interactions than by electrostatic interactions.

As mentioned above, even though the concentration of H_2SO_4 in the experiment for $Fe(bpy)_3^{2+}$ is lower than that for $Fe(ph)_3^{2+}$, the CMC of SDS for $Fe(bpy)_3^{2+}$ is higher than that for $Fe(ph)_3^{2+}$ (*i.e.* 3.38 and 2.47 mM SDS, respectively). Furthermore, the size of the $Fe(bpy)_3^{2+}$ complex is smaller than that of the $Fe(ph)_3^{2+}$ complex. However, CMC of SDS for $Fe(bpy)_3^{2+}$ is higher than that for $Fe(ph)_3^{2+}$. Also, $[Fe(bpy)_3^{2+}]$ is much smaller than $[Fe(ph)_3^{2+}]$ because $Fe(bpy)_3^{2+}$ in H_2SO_4 can be more easily decomposed than $Fe(ph)_3^{2+}$. Thus, it can be concluded that micelles can be formed more easily as the ligand of the iron complex in sulfuric acid solution changes from 2,2'-bipyridine to 1,10-phenanthroline.

References

1. Carter, M. T.; Rodriguez M.; Bard, A. J. *J. Am. Chem. Soc.* **1989**, *111*, 8901.
2. Ibel, K.; May, R. P.; Sandberg, M.; Mascher, E.; Greijer, E.; Lundahl, P. *Biophys. Chem.* **1994**, *53*, 77.
3. Yamada, S.; Hojo, K.; Yoshimura, H.; Ishikawa, K. *J. Biochem.* **1995**, *117*, 1162.
4. Dill, K. A. *et al. Nature* **1984**, *309*, 42.
5. Hartley, G. S. *Aqueous Solution of Paraffin Chain Salts*; Herman and Cie: Paris, 1936.
6. Rosen, M. J. *Surfactants and Interfacial Phenomena*; New York, 1978.
7. Fendler, J. H. *Membrane Mimetic Chemistry*; Wiley: New York, 1982.
8. Calvin, M. *Acc. Chem. Res.* **1978**, *11*, 369.
9. Kaifer, A. E.; Bard, A. J. *J. Phys. Chem.* **1985**, *89*, 4876.
10. Moulin, C.; Reiller, P.; Beaucaire, C.; Lemordant, D. *J. Colloid Interface Sci.* **1993**, *157*, 411.
11. Jaramillo, A.; Marino, A.; -Toth, A. B. Anal. Chem. **1993**, *65*, 3441.
12. Shilt, A. A. *Anal. Chem.* **1963**, *35*, 1599.
13. Kothoff, I. M. *et al. Quantitative Chemical Analysis*; The Macmillan Company: Lodon, 1969; p 758.
14. Lindman, B.; Wennerstr m, H. *Top. Curr. Chem.* **1980**, *87*, 1.
15. Ohsawa, Y.; Shimazaki, Y.; Aoyagui, S. *J. Electroanal. Chem.* **1980**, *114*, 235.
16. Mabbott, G. A. *J. Chem. Edu.* **1983**, *60*, 697.
17. Kamau, G. N.; Leipert, T.; Shukla, S. S.; Rusling, J. F. *J. Electroanal. Chem.* **1987**, *233*, 173.